

RESEARCH ACTIVITIES IX

Center for Integrative Bioscience

IX-A Molecular Mechanisms of Oxygen Activation by Heme Enzymes

By sharing a common prosthetic group, the heme enzymes such as cytochrome P450s, peroxidases, and catalases catalyze their own unique biological functions; monooxygenation, hydrogen peroxide dependent oxidation, and dismutation of hydrogen peroxide, respectively. Our efforts have been focused on the elucidation of the structure-biological function relationship of these heme enzymes by employing both enzymatic systems including mutants and their model systems.

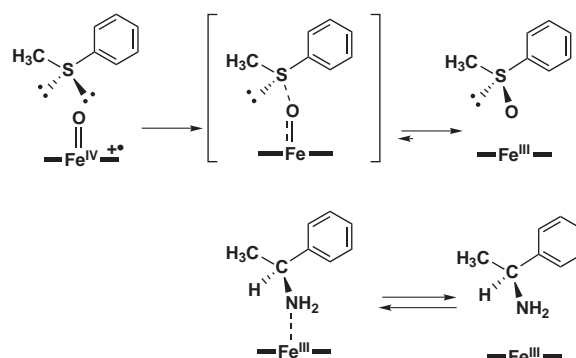
IX-A-1 Asymmetric Sulfoxidation and Amine Binding by H64D/V68A and H64D/V68S Mb: Mechanistic Insight into the Chiral Discrimination Step

KATO, Shigeru; YANG, Hui-jun; UENO, Takafumi; OZAKI, Shin-ichi¹; PHILLIPS, George N. Jr.²; FUKUZUMI, Shun-ichi³; WATANABE, Yoshihito

(¹Yamagata Univ.; ²Univ. Wisconsin; ³Osaka Univ.)

[*J. Am. Chem. Soc.* **124**, 8506 (2002)]

Myoglobin (Mb) is an oxygen transport hemoprotein that catalyzes a variety of oxidation including sulfoxidation and epoxidation in the presence of peroxides. We have recently shown that the distal histidine (His64) in sperm whale Mb is a critical residue in destabilizing a reactive intermediate, myoglobin compound I (Mb-I). The substitution of His-64 with Asp (H64D Mb) also gives Mb-I even by the reaction with H₂O₂ efficiently with the rate constant of $2.5 \times 10^4 \text{ M}^{-1}\text{s}^{-1}$. Due to the structural similarity of α -methylbenzylamine and methylphenylsulfoxide, we have examined enantioselective ligation of (*R*)- and (*S*)- α -methylbenzylamine to H64D/V68A and H64D/V68S Mbs in comparison with the sulfoxidation of thioanisole (Scheme 1). In contrast to the *R*-selective sulfoxidation by H64D/V68A and H64D/V68S, the *K* values of (*S*)- α -methylbenzylamine with H64D/V68A and H64D/V68S are 27-fold and 112-fold larger than those of the corresponding (*R*)-amine, respectively. In the case of H64D Mb, which affords almost racemic sulfoxide, however, the enantioselective binding is reversed, namely the *K* value of (*R*)-amine is about 4-fold larger than that for the (*S*) isomer.



In order to determine the chiral discrimination step in the amine binding, we have measured on rate (k_1) and off rate (k_{-1}) of amine binding to the Mb mutants by stopped-flow experiments. The on rates (k_1) of (*R*)- and (*S*)- α -methylbenzylamine to H64D/V68A and H64D/V68S are almost identical, $1.3 \times 10^4 \text{ M}^{-1}\text{s}^{-1}$ and $2.2\text{--}2.7 \times 10^4 \text{ M}^{-1}\text{s}^{-1}$, respectively. In contrast, a tremendous difference is seen for the off rate. This indicates that the chiral discrimination of the (*S*)-amine ligation over the (*R*)-amine by H64D/V68A and H64D/V68S is exclusively caused by a very small off rate of the (*S*)-amine relative to the (*R*)-amine, 1:27 for H64D/V68A and 1:92 for H64D/V68S. These selectivities would correspond to 93 and 98% ee for the amine binding, respectively. Thus, enantioselectivity in the sulfoxidation of thioanisole by H64D/V68A and H64D/V68S Mb was concluded to be determined by the off rate of sulfoxide.

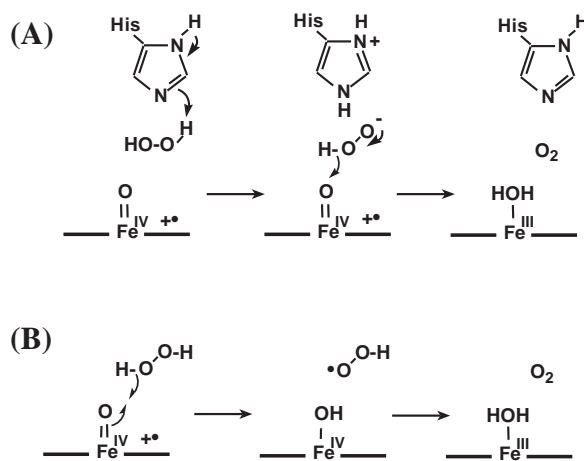
IX-A-2 Molecular Mechanism of the Catalase Reaction Studied by Myoglobin Mutants

KATO, Shigeru; UENO, Takafumi; FUKUZUMI, Shun-ichi¹; WATANABE, Yoshihito

(¹Osaka Univ.)

The catalase reaction has been studied in detail by using Mb mutants, whose compound I can be readily prepared by reaction with a nearly stoichiometric amount of *m*-chloroperbenzoic acid (*m*CPBA). Upon the addition of H₂O₂ to a Mb-I solution, Mb-I is reduced back to the ferric state without forming any intermediates. This reveals that Mb-I is capable of performing two-electron oxidation of H₂O₂ (catalatic reaction). GC-

MS analysis of the evolved O_2 from a 50:50 mixture of $H_2^{18}O_2/H_2^{16}O_2$ solution containing H64D or F43H/H64L shows two peaks for $^{18}O_2$ ($m/e = 36$) and $^{16}O_2$ ($m/e = 32$) but no indication of $^{16}O^{18}O$ ($m/e = 34$) formation. Deuterium isotope effects on rates of the catalytic reaction of Mb mutants and beef liver catalase (BLCase) suggest that the catalytic reactions of BLCase and F43H/H64L Mb proceed *via* an ionic mechanism, since the distal histidine is located at a proper position acting as a general acid-base catalyst in the ionic reaction to give a small isotope effect of less than 2.1. In contrast, other Mb mutants such as H64X (X: A, S, D) and L29H/H64L Mb oxidize H_2O_2 *via* a radical mechanism in which a hydrogen is abstracted by the ferryl species with very large isotope effects in a range of 10 to 29, due to the lack of the general acid-base catalyst. These two mechanisms are summarized in Scheme 1.



Scheme 1. Proposed mechanisms for the catalytic reaction. (A): ionic mechanism by utilizing a general acid-base catalyst. (B): Radical mechanism.

IX-B Model Studies of Non-Heme Proteins

Non-heme proteins play important roles in biological redox processes. Many reactions catalyzed by the non-heme enzymes are quite similar to those by hemoproteins. We are interested in the active intermediates responsible for oxidation and oxygenation by non-heme enzyme, especially the similarity and differences.

IX-B-1 Reactivity of Hydrogenperoxide Bound to a Mononuclear Non-Heme Iron Site

WADA, Akira¹; OGO, Seiji; NAGATOMO, Shigenori; KITAGAWA, Teizo; WATANABE, Yoshihito; JITSUKAWA, Koichiro¹; MASUDA, Hideki¹

(¹Nagoya Inst. Tech.)

[*Inorg. Chem.* **41**, 616 (2002)]

The first isolation and spectroscopic characterization of the mononuclear hydroperoxo-iron(III) complex $[Fe(H_2bppa)(OOH)]^{2+}$ (**1**) and the stoichiometric oxidation of substrates by the mononuclear iron-oxo intermediate generated by its decomposition have been described. The purple species (**1**) obtained from reaction of $[Fe(H_2bppa)(HCOO)](ClO_4)_2$ with H_2O_2 in acetone at $-50^\circ C$ gave characteristic UV-vis ($\lambda_{max} = 568$ nm, $\epsilon = 1200$ M⁻¹cm⁻¹), ESR ($g = 7.54, 5.78, \text{ and } 4.25, S = 5/2$), and ESI mass spectra (m/z 288.5 corresponding to the iron, $[Fe(bppa)(OOH)]^{2+}$), which revealed that **1** is a high-spin mononuclear iron(III) complex with a hydroperoxide in an end-on fashion. The resonance Raman spectrum of **1** in d_6 -acetone revealed two intense bands at 621 and 830 cm⁻¹, which shifted to 599 and 813 cm⁻¹, respectively, when reacted with ¹⁸O-labeled H_2O_2 . Reactions of the isolated $(bppa)Fe^{III}-OOH$ (**1**) with various substrate (single turnover oxidations) exhibited that the iron-oxo intermediate generated by decomposition of **1** is a nucleophilic species formulated as $[(H_2bppa)Fe^{III}-O\cdot]$.

IX-B-2 Synthesis, Structure, and Properties of A Novel Mononuclear Iron(III) Complex Containing Peroxocarbonate Ligand

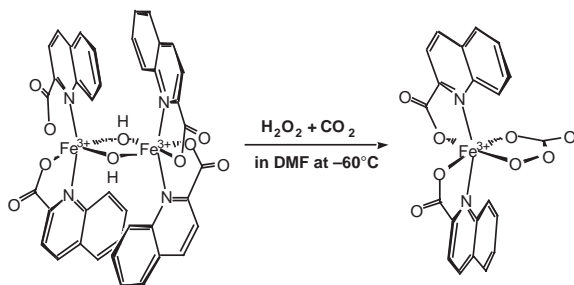
HASHIMOTO, Koji¹; NAGATOMO, Shigenori; FUJINAMI, Shuhei¹; FURUTACHI, Hideki¹; OGO, Seiji; SUZUKI, Masatatsu¹; UEHARA, Akira¹; MAEDA, Yonezo²; WATANABE, Yoshihito; KITAGAWA, Teizo

(¹Kanzawa Univ., ²Kyushu Univ.)

[*Angew. Chem. Int. Ed. Engl.* **41**, 1202 (2002)]

Mononuclear Peroxo iron(III) complexes have been proposed as a key intermediate in various oxidation reactions catalyzed by mononuclear non-heme iron enzymes and their functional model complexes. Various types of synthetic mononuclear iron(III) complexes having η^2 -peroxo, η^1 -hydroperoxo, and alkyperoxo ligand have been characterized by various spectroscopic studies. It has been shown that the structure, electronic structure, and reactivity of the peroxo complexes can be modified by the coordination environment around iron(III) center. Most of those peroxo-iron(III) complexes reported so far have nitrogen-rich coordination environments except for an edta complex. Thus it is of interest to investigate how the nature of the donor atoms and the stereochemistry of supporting ligands influence the formation, structure, and properties of such peroxo-iron(III) complexes. In this study, we have succeeded in synthesis of a mononuclear peroxocarbonate iron(III) complex with a carboxylate-rich coordination environment, $Ph_4P[Fe(qn)_2-(O_2C(O)O)] \cdot 1.5CH_3OH \cdot 0.5(CH_3)_2-$

NCHO (**1a**), derived from the reaction of a bis(μ -hydroxo)diiron(III) complex, $[\text{Fe}_2(\text{qn})_4(\text{OH})_2] \cdot 2\text{H}_2\text{O}$ (**2**) with H_2O_2 and CO_2 , where Hqn = quinaldic acid, which was characterized by X-ray, ESI-MS, EPR, UV-vis, and resonance Raman spectroscopic measurements (Scheme 1). This is the first example of a structurally characterized transition metal complex with a peroxocarbonate ligand and a mononuclear iron(III) complex having a peroxy group. We believe that the findings in this study provide an important basis for developing and expanding mononuclear iron(III) complexes having a peroxy group and are of interest to wide audience.



Scheme 1.

IX-B-3 Structural and Spectroscopic Features of a *cis* (Hydroxo)–Fe^{III}–(Carboxylato) Configuration as an Active Site Model for Lipoxigenases

OGO, Seiji¹; YAMAHARA, Ryo^{1,2}; ROACH, Mark

P.; SUENOBU, Tomoyoshi¹; AKI, Michihiko; OGURA, Takashi³; KITAGAWA, Teizo; MASUDA, Hideki²; FUKUZUMI, Shun-ichi¹; WATANABE, Yoshihito⁴

(¹Osaka Univ.; ²Nagoya Inst. Tech.; ³Univ. Tokyo; ⁴Nagoya Univ.)

[Inorg. Chem. in press]

In our preliminary communication (*Angew. Chem. Int. Ed. Engl.* **37**, 2102 (1998)), we have reported the first example of X-ray analysis of a mononuclear six-coordinate (hydroxo)iron(III) non-heme complex, $[\text{Fe}^{\text{III}}(\text{tnpa})(\text{OH})(\text{RCO}_2)]\text{ClO}_4$ {tnpa = tris(6-neopentylamino-2-pyridylmethyl)amine, **1**: $R = \text{C}_6\text{H}_5$ }, which has a characteristic *cis* (hydroxo)–Fe^{III}–(carboxylato) configuration that models the *cis* (hydroxo)–Fe^{III}–(carboxylato) moiety of the proposed (hydroxo)iron(III) species of lipoxigenases. In this full account, we report structural and spectroscopic characterization of the *cis* (hydroxo)–Fe^{III}–(carboxylato) configuration by extending the model complexes from **1** to $[\text{Fe}^{\text{III}}(\text{tnpa})(\text{OH})(\text{RCO}_2)]\text{ClO}_4$ (**2**: $R = \text{CH}_3$ and **3**: $R = \text{H}$) whose *cis* (hydroxo)–Fe^{III}–(carboxylato) moieties are isotopically labeled by $^{18}\text{OH}^-$, $^{16}\text{OD}^-$, $^{18}\text{OD}^-$, $^{12}\text{CH}_3^{12}\text{C}^{18}\text{O}_2^-$, $^{12}\text{CH}_3^{13}\text{C}^{16}\text{O}_2^-$, $^{13}\text{CH}_3^{12}\text{C}^{16}\text{O}_2^-$, $^{13}\text{CH}_3^{13}\text{C}^{16}\text{O}_2^-$, and $\text{H}^{13}\text{C}^{16}\text{O}_2^-$. Complexes **1**, **2**, and **3** are characterized by X-ray analysis, IR, EPR, and UV/Vis spectroscopy, and electrospray ionization mass spectrometry (ESI-MS).

IX-C Aqueous Organometallic Chemistry

The chemistry in aqueous media is presently undergoing very rapid growth because of many potential advantages such as alleviation of environmental problems associated with the use of organic solvents, industrial applications (*e.g.*, introduction of new biphasic processes), and reaction-specific pH selectivity. We have investigated pH-dependent reactions in aqueous media.

IX-C-1 pH-Dependent H₂-Activation Cycle Coupled to Reduction of Nitrate Ion by Cp*Ir Complexes

OGO, Seiji; NAKAI, Hidetaka; WATANABE, Yoshihito

[*J. Am. Chem. Soc.* **124**, 597 (2002)]

This paper reports a pH-dependent H₂-activation promoted by Cp*Ir complexes {Cp* = $\eta^5\text{-C}_5(\text{CH}_3)_5$ }. In a pH range of about 1 to 4, an aqueous HNO₃ solution of $[\text{Cp}^*\text{Ir}^{\text{III}}(\text{H}_2\text{O})_3]^{2+}$ (**1**) reacts with three equivalents of H₂ to yield a solution of $[(\text{Cp}^*\text{Ir}^{\text{III}})_2(\mu\text{-H})_3]^+$ (**2**) as a result of heterolytic H₂-activation. The hydrido ligands of **2** display protonic behavior and undergo H/D exchange with D⁺. Complex **2** is insoluble in a pH range of about –0.2 (1.6 M HNO₃/H₂O) to –0.8 (6.3 M HNO₃/H₂O). At pH –1 (10 M HNO₃/H₂O), a powder of **2** drastically reacts with HNO₃ to give a solution of

$[\text{Cp}^*\text{Ir}^{\text{III}}(\text{NO}_3)_2]$ (**3**) with evolution of H₂, NO, and NO₂ gases. D-labeling experiments show that the evolved H₂ is derived from the hydrido ligands of **2**. These results suggest that oxidation of the hydrido ligands of **2** couples to reduction of NO₃[–]. To complete the reaction cycle, complex **3** is transformed into **1** by increasing the pH of the solution from –1 to 1. Therefore, we are able to repeat the reaction cycle using **1**, H₂, and pH gradient between 1 and –1. A conceivable mechanism for the H₂-activation cycle with reduction of NO₃[–] is proposed.

IX-C-2 pH-Dependent Cross-Coupling Reactions of Water-Soluble Organic Halides with Organoboron Compounds Catalyzed by an Organometallic Aqua Complex $[(\text{SCS})\text{Pd}^{\text{II}}(\text{H}_2\text{O})]^+$ {SCS = C₆H₃-2,6-(CH-SBu^t)₂}

NAKAI, Hidetaka; OGO, Seiji; WATANABE, Yoshihito

[*Organometallics* **21**, 1674 (2002)]

This paper reports on the first example of pH-dependent cross-coupling reactions of water-soluble organic halides {3-*X*(C₆H₄)CO₂H, where *X* = Cl, Br, and I} with organoboron compounds {PhB(OH)₂ and Ph₄BNa} to form 3-Ph(C₆H₄)CO₂H, catalyzed by a mononuclear organometallic aqua complex [(SCS)Pd^{II}(H₂O)]₂(SO₄) {[**1**]₂·(SO₄), SCS = C₆H₃-2,6-(CH₂SBU¹)₂} in basic media (8 < pH < 13, NaHCO₃/NaOH buffers). The structure of **1**·(PF₆) was unequivocally determined by X-ray analysis. The reactions show unique pH-selectivity depending upon the organoboron compounds, *i.e.*, the rate of the reactions with PhB(OH)₂ shows a sharp maximum around pH 10, though the rate of the reactions with Ph₄BNa shows a flat maximum in a pH range of about 8 to 11. The pH-dependence is discussed on the basis of the p*K*_a values of [**1**]₂·(SO₄) and PhB(OH)₂.

IX-C-3 pH-Dependent Transfer Hydrogenation of Ketones with HCOONa as a Hydrogen Donor Promoted by (η⁶-C₆Me₆)Ru Complexes

OGO, Seiji¹; ABURA, Tsutomu; WATANABE, Yoshihito²

(¹Osaka Univ.; ²Nagoya Univ.)

[*Organometallics* **21**, 2964 (2002)]

The paper reports on the development of a new class of water-soluble organometallic catalysts for pH-dependent transfer hydrogenation. An organometallic aqua complex [(η⁶-C₆Me₆)Ru^{II}(bpy)(H₂O)]²⁺ (**1**, bpy = 2,2'-bipyridine) acts as a catalyst precursor for pH-dependent transfer hydrogenation of water-soluble and -insoluble ketones with HCOONa as a hydrogen donor in water and in biphasic media. Irrespective of the solubility of the ketones toward water, the rate of the transfer hydrogenation shows a sharp maximum around pH 4.0 (in the case of biphasic media, the pH value of the aqueous phase is adopted). In the absence of the reducible ketones, as a function of pH, complex **1** reacts with HCOONa to provide a formate complex [(η⁶-C₆Me₆)Ru^{II}(bpy)(HCOO)]⁺ (**2**) as an intermediate of β-hydrogen elimination and a hydrido complex [(η⁶-C₆Me₆)Ru^{II}(bpy)H]⁺ (**3**) as the catalyst for the transfer hydrogenation. The structures of **1**(PF₆)₂, **2**(HCOO)·HCOOH, and of [(η⁶-C₆Me₆)Ru^{II}(H₂O)₃]SO₄·3H₂O {**4**(SO₄)·3H₂O}, the starting material for the synthesis of **1**, were unequivocally determined by X-ray analysis.

IX-D Single-Molecule Physiology

A single molecule of protein (or RNA) enzyme acts as a machine which carries out a unique function in cellular activities. To elucidate the mechanisms of various molecular machines, we need to observe closely the behavior of individual molecules, because these machines, unlike man-made machines, operate stochastically and thus cannot be synchronized with each other. By attaching a tag that is huge compared to the size of a molecular machine, or a small tag such as a single fluorophore, we have been able to image the individual behaviors in real time under an optical microscope. Stepping rotation of the central subunit in a single molecule of F_1 -ATPase has been videotaped, and now we can discuss its detailed mechanism. RNA polymerase has been shown to be a helical motor that rotates DNA during transcription. Myosin V is another helical motor that moves as a left-handed spiral on the right-handed actin helix. Single-molecule physiology is an emerging field of science in which one closely watches individual, 'live' protein/RNA machines at work and examines their responses to external perturbations such as pulling and twisting. I personally believe that molecular machines operate by changing their conformations. Thus, detection of the conformational changes during function is our prime goal. Complementary use of huge and small tags is our major strategy towards this end.
<http://www.k2.ims.ac.jp/>

IX-D-1 Myosin V Is a Left-Handed Spiral Motor on the Right-Handed Actin Helix

ALI, Md. Yusuf^{1,2}; UEMURA, Sotaro³; ADACHI, Kengo¹; ITOH, Hiroyasu^{1,4}; KINOSITA, Kazuhiko, Jr.^{1,2}; ISHIWATA, Shin'ichi^{1,3}
 (¹CREST Team 13; ²Keio Univ.; ³Waseda Univ.; ⁴Hamamatsu Photonics)

[*Nature Struct. Biol.* **9**, 464 (2002)]

Myosin V is a two-headed, actin-based molecular motor implicated in organelle transport. Previously, a single myosin V molecule has been shown to move processively along an actin filament in discrete ~ 36 nm steps. However, 36 nm is the helical repeat length of actin, and the geometry of the previous experiments may have forced the heads to bind to, or halt at, sites on one side of actin that are separated by 36 nm. To observe unconstrained motion, we suspended an actin filament in solution and attached a single myosin V molecule carrying a bead duplex. The duplex moved as a left-handed spiral around the filament, disregarding the right-handed actin helix. Our results indicate a stepwise walking mechanism in which myosin V positions and orients the unbound head such that the head will land at the 11th or 13th actin subunit on the opposing strand of the actin double helix.

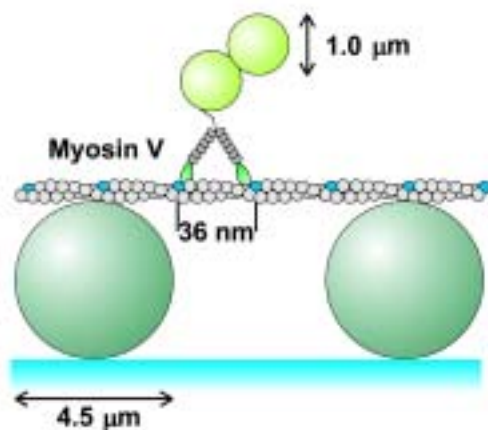


Figure 1. Experimental system for the observation of unconstrained movement of a single molecule of myosin V along an actin filament.

IX-D-2 Pause and Rotation of F_1 -ATPase during Catalysis

HIRONO-HARA, Yoko¹; NOJI, Hiroyuki^{2,3,4}; NISHIMURA, Masaya⁴; MUNAYUKI, Eiro¹; HARA, Kiyotaka Y.¹; YASUDA, Ryohei³; KINOSITA, Kazuhiko, Jr.^{3,6}; YOSHIDA, Masasuke^{1,3,5}
 (¹Tokyo Inst. Tech.; ²PRESTO; ³CREST Team 13; ⁴Univ. Tokyo; ⁵ERATO; ⁶Keio Univ.)

[*Proc. Natl. Acad. Sci. U.S.A.* **98**, 13649 (2001)]

F_1 -ATPase is a rotary motor enzyme in which a single ATP molecule drives a 120° rotation of the central γ subunit relative to the surrounding $\alpha_3\beta_3$ ring. Here, we show that the rotation of F_1 -ATPase spontaneously lapses into long (≈ 30 s) pauses during steady-state catalysis. The effects of ADP-Mg and mutation on the pauses, as well as kinetic comparison with bulk-phase catalysis, strongly indicate that the paused enzyme corresponds to the inactive state of F_1 -ATPase previously known as the ADP-Mg inhibited form in which F_1 -ATPase fails to release ADP-Mg from catalytic sites. The pausing position of the γ subunit deviates from the ATP-waiting position and is most likely the recently found intermediate 90° position.

IX-D-3 F_1 -ATPase Changes its Conformations upon Phosphate Release

MASAIKE, Tomoko¹; MUNAYUKI, Eiro¹; NOJI, Hiroyuki^{2,3}; KINOSITA, Kazuhiko, Jr.⁴; YOSHIDA, Masasuke^{1,4,5}
 (¹Tokyo Inst. Tech.; ²PRESTO; ³Univ. Tokyo; ⁴CREST Team 13; ⁵ERATO)

[*J. Biol. Chem.* **277**, 21643 (2002)]

Motor proteins, myosin, and kinesin have γ -phosphate sensors in the switch II loop that play key roles in

conformational changes that support motility. Here we report that a rotary motor, F₁-ATPase, also changes its conformations upon phosphate release. The tryptophan mutation was introduced into Arg-333 in the β subunit of F₁-ATPase from thermophilic *Bacillus* PS3 as a probe of conformational changes. This residue interacts with the switch II loop (residues 308–315) of the β subunit in a nucleotide-bound conformation. The addition of ATP to the mutant F₁ subcomplex $\alpha_3\beta$ (R333W)₃ γ caused transient increase and subsequent decay of the Trp fluorescence. The increase was caused by conformational changes on ATP binding. The rate of decay agreed well with that of phosphate release monitored by phosphate-binding protein assays. This is the first evidence that the β subunit changes its conformation upon phosphate release, which may share a common mechanism of exerting motility with other motor proteins.

IX-E Bioinorganic Chemistry of Heme-Based Sensor Proteins

Heme-based sensor proteins are a newly recognized class of heme proteins, in which the heme acts as a sensor of gaseous effector molecules such as O₂, NO, and CO. Our research interests focus on the CO-sensing transcriptional activator CooA and the O₂-sensing signal transducer HemAT. We have elucidated the structure and function relationships of CooA and HemAT by mutagenesis and some spectroscopic studies.

IX-E-1 Ligand-Switching Intermediates for the CO-Sensing Transcriptional Activator CooA Measured by Pulse Radiolysis

NAKAJIMA, Hiroshi¹; NAKAGAWA, Emi¹;
KOBAYASHI, Kazuo²; TAGAWA, Sei-ichi²;
AONO, Shigetoshi¹

(¹Japan Adv. Inst. Sci. Tech.; ²Osaka Univ.)

[*J. Biol. Chem.* **276**, 37895 (2001)]

CooA is a heme-containing and CO-sensing transcriptional activator whose activity is regulated by CO. The protoheme that acts as a CO sensor in CooA shows unique properties for its coordination structure. The Cys⁷⁵ axial ligand of the ferric heme is replaced by His⁷⁷ upon the reduction of the heme iron, and *vice versa*. In this work, the ligand-switching process induced by the reduction of the heme was investigated by the technique of pulse radiolysis. Hydrated electron reduced the heme iron in ferric CooA within 1 μs to form the first intermediate with the Soret peak at 440 nm, suggesting that a six-coordinated ferrous heme with a thiolate axial ligand was formed initially. The first intermediate was converted into the second intermediate with the time constant of 40 μs ($k = 2.5 \times 10^4 \text{ s}^{-1}$). In the second intermediate, the thiolate from Cys⁷⁵ was thought to be protonated and/or the Fe–S bond was thought to be elongated. The second intermediate was converted into the final reduced form with the time constant of 2.9 ms ($k = 3.5 \times 10^2 \text{ s}^{-1}$) for wild-type CooA. The ligand exchange between Cys⁷⁵ and His⁷⁷ took place during the conversion of the second intermediate into the final reduced form.

IX-E-2 Conformational Dynamics of the Transcriptional Regulator CooA Protein Studied by Subpicosecond Mid-Infrared Vibrational Spectroscopy

RUBTSOV, Igor V.¹; ZHANG, Tieqiao¹;
NAKAJIMA, Hiroshi¹; AONO, Shigetoshi¹;
RUBTSOV, Grigori I.²; KUMAZAKI, Shigeichi¹;
YOSHIHARA, Keitaro¹

(¹Japan Adv. Inst. Sci. Tech.; ²Lomonosov Moscow State Univ.)

[*J. Am. Chem. Soc.* **123**, 10056 (2001)]

CooA, which is a transcriptional regulator heme protein allosterically triggered by CO, is studied by femtosecond visible-pump mid-IR-probe spectroscopy. Transient bleaching upon excitation of the heme in the

Soret band is detected at approximately 1979 cm⁻¹, which is the absorption region of the CO bound to the heme. The bleach signal shows a nonexponential decay with time constants of 56 and 290 ps, caused by the rebinding of the CO to the heme. About 98% of dissociated CO recombines geminately. The geminate recombination rate in CooA is significantly faster than those in myoglobin and hemoglobin. The angle of the bound CO with respect to the porphyrin plane is calculated to be about 78 degrees on the basis of the anisotropy measurements. A shift of the bleached mid-IR spectrum of the bound CO is detected and has a characteristic time of 160 ps. It is suggested that the spectral shift is caused by a difference in the frequency of the bound CO in different protein conformations, particularly in an active conformation and in an intermediate one, which is on the way toward an inactive conformation. Thus, the biologically relevant conformation change in CooA was traced. Possible assignment of the observed conformation change is discussed.

IX-E-3 Resonance Raman and Ligand Binding Studies of the Oxygen Sensing Signal Transducer Protein HemAT from *Bacillus subtilis*

AONO, Shigetoshi¹; KATO, Toshiyuki¹; MATSUKI, Mayumi¹; NAKAJIMA, Hiroshi¹; OHTA, Takehiro;
UCHIDA, Takeshi; KITAGAWA, Teizo

(¹Japan Adv. Inst. Sci. Tech.)

[*J. Biol. Chem.* **277**, 13528 (2002)]

HemAT-Bs is a heme-containing signal transducer protein responsible for aerotaxis of *Bacillus subtilis*. The recombinant HemAT-Bs expressed in *E. coli* was purified as the oxy form in which oxygen was bound to the ferrous heme. Oxygen binding and dissociation rate constants were determined to be $k_{\text{on}} = 32 \mu\text{M}^{-1}\text{s}^{-1}$ and $k_{\text{off}} = 23 \text{ s}^{-1}$, respectively, revealing that HemAT-Bs has a moderate oxygen affinity similar to that of sperm whale Mb. The rate constant for autoxidation at 37 °C was 0.06 h⁻¹, which is also close to that of Mb. Although the electronic absorption spectra of HemAT-Bs were similar to those of Mb, HemAT-Bs showed some unique characteristics in its resonance Raman spectra. Oxygen-bound HemAT-Bs gave the $\nu(\text{Fe}-\text{O}_2)$ band at a noticeably low frequency (560 cm⁻¹), which suggests a unique hydrogen bonding between a distal amino acid residue and the proximal atom of the bound oxygen molecule. Deoxy HemAT-Bs gave the $\nu_{\text{Fe}-\text{His}}$ band at a higher frequency (225 cm⁻¹) than those of ordinary His-coordinated deoxy heme proteins. CO-bound HemAT-

Bs gave the $\nu(\text{Fe-CO})$ and $\nu(\text{C-O})$ bands at 494 and 1964 cm^{-1} , respectively, which fall on the same $\nu(\text{C-O})$ vs $\nu(\text{Fe-CO})$ correlation line as that of Mb. Based on these results, the structural and functional properties of HemAT-Bs are discussed.

IX-F Electronic Structure and Reactivity of Active Sites of Metalloproteins

Metalloproteins are a class of biologically important macromolecules that have various functions such as oxygen transport, electron transfer, oxidation, and oxygenation. These diverse functions of metalloproteins have been thought to depend on the ligands from amino acids, coordination structures, and protein structures in immediate vicinity of metal ions. In this project, we are studying the relationship between the structures of the metal active sites and functions of metalloproteins.

IX-F-1 Trigonal Bipyramidal Ferric Aqua Complex with Sterically Hindered Salen Ligand as a Model for Active Site of Protocatechuate 3,4-Dioxygenase

FUJII, Hiroshi; FUNAHASHI, Yasuhiro

[*Angew. Chem. Int. Ed. Engl.* in press]

Protocatechurate 3,4-dioxygenase (3,4-PCD) has been found in soil bacteria and is known to play a role in degrading aromatic molecules in nature. The enzyme is classified as an intradiol dioxygenase and cleaves catechol analogues bound to the iron(III) site into aliphatic products with incorporation of both atoms of molecular oxygen. It has been proposed that the enzyme does not activate an iron-bound oxygen molecule, but rather induces an iron-bound catecholate to react with O₂. Therefore, knowledge of the structure and electronic state of the iron site is essential to understanding the unique reaction of 3,4-PCD. A previous crystal structure analysis of 3,4-PCD from *Pseudomonas putida* revealed a distorted trigonal-bipyramidal ferric iron center with four endogenous protein ligands (Tyr 408, Tyr 447, His 460, and His 462) and a solvent-derived water molecule (see Figure 2). To understand the structure-function relationship of 3,4-PCD, attempts have been made over several decades to prepare inorganic model complexes of 3,4-PCD. However, no iron(III) complex that reproduces the active site of 3,4-PCD has been characterized. We report here the first example of a distorted trigonal-bipyramidal ferric aqua complex with a sterically hindered salen ligand that not only duplicates the active site but also mimics the spectral characteristics of 3,4-PCD.

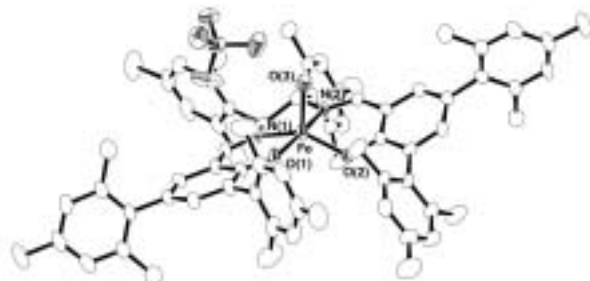


Figure 1. Structure of 3,4-PCD active site model complex prepared in this project.

IX-F-2 ¹³C-NMR Signal Detection of Iron Bound Cyanide Ions in Ferric Cyanide Complexes of Heme Proteins

FUJII, Hiroshi

[*J. Am. Chem. Soc.* **124**, 5936 (2002)]

Small molecule axial ligands potentially can serve as useful NMR probes for characterization of environment and electronic structure of prosthetic group in heme protein. In this regard, the diamagnetic ferrous states have been examined thoroughly because of easy signal detection from iron bound small molecule. The ¹³C-NMR signal of ¹³CO form of heme protein proves to be sensitive to the nature of the trans amino acid ligand. For the paramagnetic ferric state, cyanide ion would appear to have the greatest potential because of its extremely high affinity to ferric heme iron center. ¹⁵N-NMR signals of the iron bound C¹⁵N have been detected in a far-downfield region for both iron(III) porphyrin model complexes and heme proteins. However, the ¹⁵N-NMR spectroscopy remains ambiguity as a NMR probe since the ¹⁵N-NMR shift reflects the nature of both hydrogen bond in the distal side and amino acid ligand in the proximal side. On the other hand, ¹³C-NMR spectroscopy of the iron bound ¹³CN has been investigated in less detail. Although ¹³C-NMR signals of the iron bound ¹³CN are detectable in a far-upfield region (~ -2500 ppm from TMS) for bis-cyanide iron(III) porphyrin model complexes, extreme line-broadening of the signal seemed to preclude the signal detection in heme proteins and a resonance of the iron bound ¹³CN for ferric heme protein has not yet been located. During a more extensive ¹³C-NMR study, we found the ¹³C-NMR signals of the iron bound ¹³CN of ferric cyanide complexes of heme proteins and its model complexes at an unexpectedly large upfield region (~ -4000 ppm from TMS). Here, we report the first detection of ¹³C-NMR signal of the iron bound ¹³CN in heme proteins such as sperm whale myoglobin(Mb), human hemoglobin(Hb), horse heart cytochrome *c*(Cyt-*c*), and horseradish peroxidase(HRP). This study shows that the ¹³C-NMR spectroscopy of the iron bound ¹³CN provides a probe for studying nature of the proximal ligand in ferric heme protein.

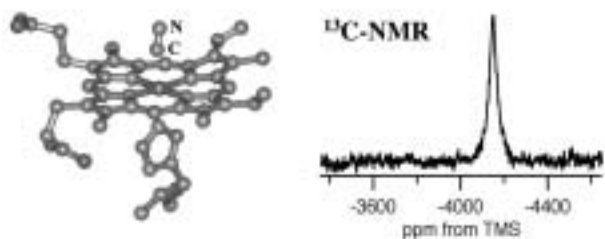


Figure 1. Active site structure of cyanide form of ferric heme protein and its ^{13}C -NMR spectrum.

IX-G Molecular Mechanism of Heme Degradation and Oxygen Activation by Heme Oxygenase

Heme oxygenase (HO), an amphipathic microsomal proteins, catalyzes the regiospecific oxidative degradation of iron protoporphyrinIX (heme) to biliverdinIX α , carbon monoxide, and iron in the presence of NADPH-cytochrome P-450 reductase, which functions as an electron donor. Heme oxygenase reaction is the biosynthesis processes of bile pigments and CO, which is a possible physiological messenger. Recent development in the bacterial expression of a soluble form of heme oxygenase has made it possible to prepare in the large quantities for structural studies. In this project, we are studying the molecular mechanism of heme degradation and the oxygen activation by heme oxygenase using various spectroscopic methods.

IX-G-1 Catalytic Mechanism of Heme Oxygenase through EPR and ENDOR of Cryoreduced Oxy-Heme Oxygenase and Asp 140 Mutants

DAVYDOV, Roman¹; KOFMAN, Viktoria¹; FUJII, Hiroshi; YOSHIDA, Tadashi²; IKEDA-SAITO, Masao³; HOFFMAN, M. Brian¹
(¹Uni. Northweatern; ²Yamagata Univ.; ³Tohoku Univ.)

annealing of wild-type oxy-HO and D140A, F mutants.

[*J. Am. Chem. Soc.* **124**, 1798 (2002)]

Heme oxygenase (HO) catalyzes the O₂- and NADPH-cytochrome P450 reductase-dependent conversion of heme to biliverdin and CO through a process in which the heme participates both as prosthetic group and substrate. It was proposed that the first mono-oxygenation step of HO catalysis is the conversion of the heme to a-meso-hydroxyheme, through a process in which an electron provided by NADPH-cytochrome P450 reductase reduces the first heme to the ferrous state and molecular of dioxygen binds to form a metastable O₂-bound complex, which then is reduced by a second electron to generate hydroperoxy ferric-HO. It was further thought that the hydroperoxy-ferric HO is the reactive hydroxylating species, rather than a high-valent ferryl active intermediate as in the case of cytochrome P450cam. However, neither the putative hydroperoxy-ferric-HO intermediate nor the a-meso-hydroxyheme product had been detected during physiological HO catalysis until our recent EPR and ENDOR study of oxy-ferrous HO cryoreduced at 77 K. In the present study we have generated a detailed reaction cycles for the first mono-oxygenation step of HO catalysis. We employed EPR and ¹H, ¹⁴N ENDOR spectroscopies to characterize the intermediates generated by 77 K radiolytic cryoreduction and subsequent

IX-H Biomolecular Science

Elucidation of a structure-function relationship of metalloproteins is a current subject of this group. The primary technique used for this project is the stationary and time-resolved resonance Raman spectroscopy excited by visible and UV lasers. The main themes that we want to explore are (1) mechanism of oxygen activation by enzymes, (2) mechanism of active proton translocation and its coupling with electron transfer, (3) coupling mechanism of proton- and electron transfers by quinones in photosynthetic reaction center, (4) higher order protein structures and their dynamics, and (5) reactions of biological NO. In category (1), we have examined a variety of terminal oxidases, cytochrome P450s, and peroxidases, and also treated their enzymatic reaction intermediates by using the mixed flow transient Raman apparatus and the Raman/absorption simultaneous measurement device. For (2) the third generation UV resonance Raman (UVR) spectrometer was constructed and we are going to apply it to a giant protein like cytochrome c oxidase. More recently, we succeeded in pursuing protein folding of apomyoglobin by combining UV time-resolved Raman and rapid mixing device. In (3) we succeeded in observing RR spectra of quinones A and B in bacterial photosynthetic reaction centers for the first time, but we have focused our attention on detecting tyrosine radical for the P intermediate of terminal oxidases. Some positive evidence was obtained for cytochrome *bo*. For (4) we developed a novel technique for UV resonance Raman measurements based on the combination of the first/second order dispersions of gratings and applied it successfully to 235-nm excited RR spectra of several proteins including mutant hemoglobins and myoglobins. Nowadays we can carry out time-resolved UVR experiments with nanosecond resolution to discuss protein dynamics. With the newly developed third generation UV Raman spectrometer, we have succeeded in isolating the spectrum of tyrosinate in ferric Hb M Iwate, which was protonated in the ferrous state, and the deprotonated state of Tyr244 of bovine cytochrome c oxidase. As a model of Tyr244, an imidazole-bound *para*-cresol was synthesized and its UV resonance Raman was investigated. For (5) we purified soluble guanylate cyclase from bovine lung and observed its RR spectra. To further investigate it, we are developing an expression system of this protein.

IX-H-1 Stationary and Time-Resolved Resonance Raman Spectra of His77 and Met95 Mutants of the Isolated Heme Domain of a Direct Oxygen Sensor from *E. coli*

SATO, Akira¹; SASAKURA, Yukie²; SUGIYAMA, Shunpei²; SAGAMI, Ikuko²; SHIMIZU, Toru²; MIZUTANI, Yasuhisa³; KITAGAWA, Teizo
(¹GUAS; ²Tohoku Univ.; ³Kobe Univ.)

[*J. Biol. Chem.* **277**, 32650 (2002)]

The heme environments of Met95 and His77 mutants of the isolated heme-bound PAS domain (*Ec* DOS PAS) of a direct oxygen sensing protein from *E. coli* (*Ec* Dos) were investigated with resonance Raman (RR) spectroscopy and compared to the wild type enzyme (WT). The RR spectra of both the reduced and oxidized WT enzyme were characteristic of six-coordinated low-spin heme complexes from pH 4 to 10. The time-resolved RR spectra of the photo-dissociated CO-WT complex had an Fe-His stretching band ($\nu_{\text{Fe-His}}$) at 214 cm^{-1} , and the $\nu_{\text{Fe-CO}}$ vs ν_{CO} plot of CO-WT *Ec* DOS PAS fell on the line of His-coordinated heme proteins. The photo-dissociated CO-His77Ala mutant complex did not yield the $\nu_{\text{Fe-His}}$ band but gave a $\nu_{\text{Fe-Im}}$ band in the presence of imidazole. The RR spectrum of the oxidized Met95Ala mutant was that of a six-coordinated low-spin complex, *i.e.* the same as that of the WT enzyme, whereas the reduced mutant appeared to contain a five-coordinated heme complex. Taken together, we suggest that the heme of the reduced WT enzyme is coordinated by His77 and Met95, and that Met95 is displaced by CO and O₂. Presumably, the protein conformational change that occurs on exchange of an unknown ligand for Met95 following heme reduction, may lead to activation of the phosphodi-

esterase domain of *Ec* Dos.

IX-H-2 Resonance Raman Studies on Xanthine Oxidase: Observation of the Mo^{VI}-Ligand Vibration

MAITI, Nakul C.¹; OKAMOTO, Ken²; NISHINO, Takeshi²; TOMITA, Takeshi³; KITAGAWA, Teizo
(¹CIB and Case Western Reserve Univ.; ²Nippon Medical School; ³CIB and Tohoku Univ.)

[*J. Biol. Inorg. Chem.* in press]

Resonance Raman spectra were investigated for the sulfo- and desulfo-forms of cow's milk xanthine oxidase with various visible excitation lines between 400 and 650 nm, and the Mo^{VI}-ligand vibrations were observed for the first time. The Mo^{VI}=S stretch was identified at 474 and 462 cm^{-1} for the ³²S and ³⁴S-sulfo-forms, respectively, but was absent in the reduced state and in the desulfo form. The Mo^{VI}=O stretch was weakly observed at 899 cm^{-1} for the sulfo-form and shifted to 892 cm^{-1} with very weak intensity for the dioxo desulfo-form. In measurements of an excitation profile, the two bands at 474 and 899 cm^{-1} showed maximum intensity at similar excitation wavelengths, suggesting that the Raman intensity of the metal-ligand modes is owed to the Mo^{VI} ← S CT transition, and that this is the origin of the intrinsically weak features of the Mo^{VI}-ligand Raman bands. When the sulfo-form was regenerated from the desulfo-form, the 899 cm^{-1} band reappeared. However, the band at 899 cm^{-1} showed no frequency shift when regeneration was conducted in H₂¹⁸O, or after several turnovers in the presence of xanthine in H₂¹⁸O. When the sulfo-form was reduced and reoxidized in H₂¹⁸O buffer, the 899 cm^{-1} band reappeared without any frequency shift. These observa-

tions suggest that the oxo oxygen in the Mo center of xanthine oxidase is not labile. Low-frequency vibrations of the Mo-center were observed together with those of the Fe₂S₂ center with some overlaps, while FAD modes were observed clearly. The absence of dithiolene modes in XO is in contrast to the Mo^V-centers of DMSO reductase and sulfite oxidase.

IX-H-3 Changes in the Abnormal α -Subunit upon CO-Binding to the Normal β -Subunit of Hb M Boston: Resonance Raman, EPR, and CD Study

NAGATOMO, Shigenori; JIN, Yayoi¹; NAGAI, Masako¹; HORI, Hiroshi²; KITAGAWA, Teizo (¹Kanazawa Univ.; ²Osaka Univ.)

[*Biophys. Chem.* **98**, 217 (2002)]

Heme-heme interaction in Hb M Boston (His α 58 \rightarrow Tyr) was investigated with visible and UV resonance Raman (RR), EPR, and CD spectroscopies. Although Hb M Boston has been believed to be frozen in the *T* quaternary state, oxygen binding exhibited appreciable cooperativity ($n = 1.4$) and the near-UV CD spectrum indicated weakening of the *T* marker at pH 9.0. Binding of CO to the normal β subunit gave no change in the EPR and visible Raman spectra of the abnormal α subunit at pH 7.5, but it caused an increase of EPR rhombicity and significant changes in the Raman coordination markers as well as the Fe(III)-tyrosine related bands of the α subunit at pH 9.0. The UVRR spectra indicated appreciable changes of Trp but not of Tyr upon CO binding to the β subunit at pH 9.0. Therefore, we conclude that the ligand binding to the β heme induces quaternary structure change at pH 9.0 and is communicated to the α heme presumably through His β 92 \rightarrow Trp β 37 \rightarrow His α 87.

IX-H-4 Coordination Geometry of Cu-Porphyrin in Cu(II)-Fe(II) Hybrid Hemoglobins Studied by Q-Band EPR and Resonance Raman Spectroscopies

VENKATESH, Balan¹; HORI, Hiroshi¹; MIYAZAKI, Gentaro¹; NAGATOMO, Shigenori; KITAGAWA, Teizo; MORIMOTO, Hideki¹ (¹Osaka Univ.)

[*J. Inorg. Biochem.* **88**, 310 (2002)]

Cu(II)-Fe(II) hybrid hemoglobins were investigated by UV-vis, Q-band (35 GHz) EPR and resonance Raman spectroscopies. EPR results indicated that Cu-porphyrin in α -subunit within hybrid hemoglobin had either 5- or 4-coordination geometry depending on the pH conditions, while Cu-porphyrin in β -subunit had only 5-coordination geometry at high and low pH values. These results were consistent with UV-vis absorption results. A new resonance Raman band appeared around 190 cm⁻¹, which was present whenever 5-coordinated Cu-porphyrin existed in Cu(II)-Fe(II) hybrid hemoglobins irrespective of the coordination number in Fe(II) subunit. This Raman band might be

assigned to Cu-His stretching mode. These results are direct demonstration of the existence of coordination changes of Cu-porphyrin in α -subunit within hybrid hemoglobin by shifting the molecular conformation from fully unliganded state to intermediately liganded state.

IX-H-5 Fine-Tuning of Copper(I)-Dioxygen Reactivity by 2-(2-Pyridyl)ethylamine Bidentate Ligands

TAKI, Masayasu¹; TERAMAE, Shinichi¹; NAGATOMO, Shigenori; TACHI, Yoshimitsu²; KITAGAWA, Teizo; ITOH, Shinobu²; FUKUZUMI, Shun-ichi¹ (¹Osaka Univ.; ²Osaka City Univ.)

[*J. Am. Chem. Soc.* **124**, 6367 (2002)]

Copper(I)-dioxygen reactivity has been examined using a series of 2-(2-pyridyl)ethylamine bidentate ligands ^{R1}Py1^{R2,R3}. The bidentate ligand with the methyl substituent on the pyridine nucleus ^{Me}Py1^{Et,Bz} (*N*-benzyl-*N*-ethyl-2-(6-methylpyridin-2-yl)ethylamine) predominantly provided a (μ - η^2 : η^2 -peroxo)dicopper(II) complex, while the bidentate ligand without the 6-methyl group ^HPy1^{Et,Bz} (*N*-benzyl-*N*-ethyl-2-(2-pyridyl)ethylamine) afforded a bis(μ -oxo)dicopper(III) complex under the same experimental conditions. Both Cu₂O₂ complexes gradually decompose, leading to oxidative *N*-dealkylation reaction of the benzyl group. Detailed kinetic analysis has revealed that the bis(μ -oxo)dicopper(III) complex is the common reactive intermediate in both cases and that O-O bond homolysis of the peroxo complex is the rate-determining step in the former case with ^{Me}Py1^{Et,Bz}. On the other hand, the copper(I) complex supported by the bidentate ligand with the smallest *N*-alkyl group (^HPy1^{Me,Me}, *N,N*-dimethyl-2-(2-pyridyl)ethylamine) reacts with molecular oxygen in a 3:1 ratio in acetone at a low temperature to give a mixed-valence trinuclear copper(II, II, III) complex with two μ_3 -oxo bridges, the UV-vis spectrum of which is very close to that of an active oxygen intermediate of lacase. Detailed spectroscopic analysis on the oxygenation reaction at different concentrations has indicated that a bis(μ -oxo)dicopper(III) complex is the precursor for the formation of trinuclear copper complex. In the reaction with 2,4-di-*tert*-butylphenol (DBP), the trinuclear copper(II, II, III) complex acts as a two-electron oxidant to produce an equimolar amount of the C-C coupling dimer of DBP (3,5,3',5'-tetra-*tert*-butyl-biphenyl-2,2'-diol) and a bis(μ -hydroxo)dicopper(II) complex. Kinetic analysis has shown that the reaction consists of two distinct steps, where the first step involves a binding of DBP to the trinuclear complex to give a certain intermediate that further reacts with the second molecule of DBP to give another intermediate, from which the final products are released. Steric and/or electronic effects of the 6-methyl group and the *N*-alkyl substituents of the bidentate ligands on the copper(I)-dioxygen reactivity have been discussed.

IX-H-6 Modulation of the Copper-Dioxygen Reactivity by Stereochemical Effect of Tetradentate Tripodal Ligands

HAYASHI, Hideki¹; UOZUMI, Kounosuke¹; FUJINAMI, Shuhei¹; NAGATOMO, Shigenori; SHIREN, Kazushi¹; FURUTACHI, Hideki¹; SUZUKI, Masatatsu¹; UEHARA, Akira¹; KITAGAWA, Teizo
(¹Kanazawa Univ.)

[*Chem. Lett.* 416 (2002)]

Dioxygen reactivity of a copper(I) complex having a sterically hindered Me-3-tpa and monooxygenase activity of its oxygenated species toward the ligand were significantly modulated by the presence of the 6-methyl group onto pyridyl group.

IX-H-7 Reactivity of Hydroperoxide Bound to a Mononuclear Non-Heme Iron Site

WADA, Akira¹; OGO, Seiji; NAGATOMO, Shigenori; KITAGAWA, Teizo; WATANABE, Yoshihito; JITSUKAWA, Koichiro¹; MASUDA, Hideki¹
(¹Nagoya Inst. Tech.)

[*Inorg. Chem.* **41**, 616 (2002)]

The first isolation and spectroscopic characterization of the mononuclear hydroperoxo-iron(III) complex [Fe(H₂bppa)(OOH)]²⁺ (**2**) and the stoichiometric oxidation of substrates by the mononuclear iron-oxo intermediate generated by its decomposition have been described. The purple species **2** obtained from reaction of [Fe(H₂bppa)(HCOO)](ClO₄)₂ with H₂O₂ in acetone at -50 °C gave characteristic UV-vis (λ_{max} = 568 nm, ϵ = 1200 M⁻¹cm⁻¹), ESR (g = 7.54, 5.78, and 4.25, S = 5/2), and ESI mass spectra (m/z 288.5 corresponding to the ion, [Fe(bppa)(OOH)]²⁺, which revealed that **2** is a high-spin mononuclear iron(III) complex with a hydroperoxide in an end-on fashion. The resonance Raman spectrum of **2** in *d*₆-acetone revealed two intense bands at 621 and 830 cm⁻¹, which shifted to 599 and 813 cm⁻¹, respectively, when reacted with ¹⁸O-labeled H₂O₂. Reactions of the isolated (bppa)Fe^{III}-OOH (**2**) with various substrates (single turnover oxidations) exhibited that the iron-oxo intermediate generated by decomposition of **2** is a nucleophilic species formulated as [(H₂bppa)Fe^{III}-O[•]].

IX-H-8 A New Mononuclear Iron(III) Complex Containing a Peroxocarbonate Ligand

HASHIMOTO, Koji¹; NAGATOMO, Shigenori; FUJINAMI, Shuhei¹; FURUTACHI, Hideki¹; OGO, Seiji; SUZUKI, Masatatsu¹; UEHARA, Akira¹; MAEDA, Yonezo²; WATANABE, Yoshihito; KITAGAWA, Teizo
(¹Kanazawa Univ.; ²Kyushu Univ.)

[*Angew. Chem. Int. Ed. Engl.* **41**, 1205 (2002)]

Stabilization of a peroxocarbonate ligand by formation of a five-membered chelate ring. The mononuclear peroxocarbonate complex **1** was prepared by the reaction of a bis(μ -hydroxo)diiron(III) complex with H₂O₂ and CO₂. Compound **1** is the first crystallography characterized transition metal complex with a peroxocarbonate ligand. Formation of the peroxocarbonate moiety in **1** proceeds by a nucleophilic addition of a peroxide anion to CO₂. Hqn = quinaldic acid.

IX-H-9 Formation, Characterization, and Reactivity of Bis(μ -oxo)dinickel(III) Complexes Supported by a Series of Bis[2-(2-pyridyl)ethyl]amine Ligands

ITOH, Shinobu¹; BANDO, Hideki²; NAKAGAWA, Motonobu²; NAGATOMO, Shigenori; KITAGAWA, Teizo; KARLIN, Kenneth D.³; FUKUZUMI, Shun-ichi²
(¹Osaka City Univ.; ²Osaka Univ.; ³Johns Hopkins Univ.)

[*J. Am. Chem. Soc.* **123**, 11168 (2001)]

Bis(μ -oxo)dinickel(III) complexes supported by a series of bis[2-(2-pyridyl)ethyl]amine ligands have been successfully generated by treating the corresponding bis(μ -hydroxo)dinickel(II) complexes or bis(μ -methoxo)dinickel(II) complex with an equimolar amount of H₂O₂ in acetone at low temperature. The bis(μ -oxo)dinickel(III) complexes exhibit a characteristic UV-vis absorption band at ~ 410 nm and a resonance Raman band at 600–610 cm⁻¹ that shifted to 570–580 cm⁻¹ upon ¹⁸O-substitution. Kinetic studies and isotope labeling experiments using ¹⁸O₂ imply the existence of intermediate(s) such as peroxo dinickel(II) in the course of formation of the bis(μ -oxo)dinickel(III) complex. The bis(μ -oxo)dinickel(III) complexes supported by the mononucleating ligands (**L1**^X = para-substituted *N,N*-bis[2-(2-pyridyl)ethyl]-2-phenylethylamine; X = OMe, Me, H, Cl) gradually decompose, leading to benzylic hydroxylation of the ligand side arm (phenethyl group). The kinetics of the ligand hydroxylation process including kinetic deuterium isotope effects (KIE), *p*-substituent effects (Hammett plot), and activation parameters ($\Delta H_{\text{H}}^{\ddagger}$ and $\Delta S_{\text{H}}^{\ddagger}$) indicate that the bis(μ -oxo)dinickel(III) complex exhibits an ability of hydrogen atom abstraction from the substrate moiety as in the case of the bis(μ -oxo)dicopper(III) complex. Such a reactivity of bis(μ -oxo)dinickel(III) complexes has also been suggested by the observed reactivity toward external substrates such as phenol derivatives and 1,4-cyclohexadiene. The thermal stability of the bis(μ -oxo)dinickel(III) complex is significantly enhanced when the dinucleating ligand with a longer alkyl strap is adopted instead of the mononucleating ligand. In the *m*-xylyl ligand system, no aromatic ligand hydroxylation occurred, showing a sharp contrast with the reactivity of the (μ - η^2 : η^2 -peroxo)dicopper(II) complex with the same ligand which induces aromatic ligand hydroxylation via an electrophilic aromatic substitution mechanism. Differences in the structure and reactivity of the active oxygen complexes between the nickel and the copper systems are discussed on the basis of the detailed

comparison of these two systems with the same ligand.

IX-H-10 UV Resonance Raman and NMR Spectroscopic Studies on the pH Dependent Metal Ion Release from Pseudoazurin

SATO, Katsuko¹; NAGATOMO, Shigenori;
DENNISON, Christopher²; NIIZEKI, Tomotake¹;
KITAGAWA, Teizo; KOHZUMA, Takamitsu¹
(¹Ibaraki Univ.; ²Univ. Newcastle upon Tyne)

[*Inorg. Chim. Acta* in press]

UV resonance Raman (UVRR) and ¹H NMR spectra are measured for native Cu(I)- and Cu(II)-pseudoazurin, its apo-protein, and a few metal-substituted derivatives. The pH titration experiments of ¹H NMR enabled us to determine the pK_a^{*} values of three His residues (His6, His40, and His81). The UVRR band characteristic of a metal coordinated histidyl imidazole was observed at 1385 cm⁻¹ for Cu(II)-pseudoazurin in D₂O but not for Cu(I)-pseudoazurin. This frequency is consistent with the N_δ coordination of His. For the Cu(I)-pseudoazurin

a characteristic band of histidyl imidazolium was detected at 1408 cm⁻¹ at acidic pH. This is assigned to protonated His81, which is deligated from Cu(I) at low pH values. The imidazolium Raman band at 1408 cm⁻¹ was also detected in the UVRR spectrum of apo-pseudoazurin at pH* = 3.9, and the acidification was accompanied by a significant change in the X-Pro bands at 1467 cm⁻¹. Pseudoazurin substituted with Zn²⁺ and Cd²⁺ gave the characteristic Raman bands of the metal coordinated imidazole at 1388 and 1384 cm⁻¹, respectively, at neutral pH, but its intensity diminished upon lowering the pH, and instead the imidazolium band at 1408 cm⁻¹ grew. The X-Pro bands of the pseudoazurins substituted with Zn²⁺ and Cd²⁺ exhibited the pH dependence very similar to that observed for apo-pseudoazurin. These findings indicate that the Zn²⁺ and Cd²⁺ ions are released from the active site at acidic pH and it is accompanied by a change in hydrogen bonding state of Pro80. This behavior is clearly absent in both the Cu(I) and Cu(II) proteins, meaning that pseudoazurin discriminates between copper and the other metal ions.

IX-I Fast Dynamics of Photoproducts in Solution Phases

Picosecond time-resolved resonance Raman (ps-TR³) spectroscopy is a promising technique to investigate ultrafast structural changes of molecules. However, this technique has not been used as widely as nanosecond TR³ spectroscopy, mainly due to the lack of light source which has suitable repetition rates of pulses and wavelength tunability. In order to obtain qualified TR³ spectra, first we need two independently tunable light sources for pump and probe pulses. Second, the repetition rate should be higher than kiloHertz to keep a moderate average laser power without making the photon density of probe pulse too high. We succeeded in developing light sources for ps-TR³ spectroscopy having wide tunability and kHz repetition, and applied them to study fast dynamics of photo-excited molecules. For carbonmonoxy myoglobin (MbCO), vibrational relaxation with the time constant of 1.9 ps was observed for CO-photodissociated heme. For Ni-octaethylporphyrin in benzene, differences in rise times of population in vibrationally excited levels among various modes were observed in the anti-Stokes spectra for the first time. This technique has been applied to identify the trans ligand of CO in the CO-bound transcriptional factor, Coo A.

On the other hand, we have constructed a nanosecond temperature-jump apparatus using a water absorption in near infrared. The new apparatus based on a Nd:YAG laser was combined with a time-resolved Raman measurement system and applied successfully to explore thermal unfolding of ribonuclease A.

IX-I-1 Time-Resolved Resonance Raman Study on Ultrafast Structural Relaxation and Vibrational Cooling of Photodissociated Carbonmonoxy Myoglobin

KITAGAWA, Teizo; HARUTA, Nami; MIZUTANI, Yasuhisa

[*Biopolymers (Biospectroscopy)* **67**, 207 (2002)]

A localized small structural change is converted to a higher order conformational change of protein and extends to a mesoscopic scale to induce a physiological function. To understand such features of protein, ultrafast dynamics of myoglobin (Mb) following CO photolysis have been investigated in this laboratory. Recent results are summarized here with a stress on

structural and vibrational energy relaxation. The core expansion of heme takes place within 2 ps but the out-of-plane displacement of the heme iron and the accompanied protein conformational change occur in ~10 and ~100 picosecond regimes, respectively. It was found from UV resonance Raman spectra that Trp7 in the N-terminal region and Tyr151 in the C-terminal region undergo appreciable structural changes upon ligand binding/dissociation and as a result, the rate of spectral change of iron-histidine (Fe-His) stretching band is influenced by viscosity of solvent. Temporal changes of the anti-Stokes Raman intensity demonstrated immediate generation of vibrationally excited heme upon photodissociation and its decay with a time constant of 1.1 ps.

IX-I-2 Vibrational Energy Relaxation of Metalloporphyrins in a Condensed Phase Probed by Time-Resolved Resonance Raman Spectroscopy

MIZUTANI, Yasuhisa; KITAGAWA, Teizo

[*Bull. Chem. Soc. Jpn.* **75**, 623 (2002)]

Recent experimental work on vibrational energy relaxation of metalloporphyrins in a condensed phase carried out in this laboratory is summarized. The formation of a vibrationally excited photoproduct of metalloporphyrins upon (π , π^*) excitation and its subsequent vibrational energy relaxation were monitored by picosecond time-resolved resonance Raman spectroscopy. Results related to intramolecular relaxation of octaethylporphyrinato nickel (NiOEP) are described. Stokes Raman bands due to a photoproduct of NiOEP instantaneously appeared upon the photoexcitation. Their intensities decayed with a time constant of ~ 300 ps, which indicates an electronic relaxation from the (d , d) excited state (B_{1g}) to the ground state (A_{1g}), being consistent with the results of transient absorption measurements. Anti-Stokes ν_4 and ν_7 bands for vibrationally excited (d , d) state of NiOEP decayed with time constants of ~ 10 and ~ 300 ps. The former is ascribed to vibrational relaxation, while the latter corresponds to the electronic relaxation from the (d , d) excited state to the electronic ground state. While the rise of anti-Stokes ν_4 intensity was instrument-limited, the rise of anti-Stokes ν_7 intensity was delayed by 2.0 ± 0.4 ps, which indicates that intramolecular vibrational energy redistribution has not been completed in the subpicosecond time regime. To study the mechanism of intermolecular energy transfer, solvent dependence of the time constants of anti-Stokes kinetics was investigated using various solvents. No significant solvent dependence of the rise and decay constants was observed for NiOEP. For an iron porphyrin, we observed two phases in intermolecular energy transfer. The fast phase was insensitive to solvent and the slow phase depended on solvents. A model of classical thermal diffusion qualitatively reproduced this behavior. For myoglobin, temporal changes of the anti-Stokes Raman intensity of the ν_4 and ν_7 bands demonstrated immediate generation of a vibrationally excited heme upon photodissociation and subsequent decays of the excited populations, whose time constants were 1.1 ± 0.6 and 1.9 ± 0.6 ps, respectively. This direct monitoring of the cooling dynamics of the heme cofactor within the protein matrix allows the characterization of the vibrational energy flow through the protein moiety and to the water bath. For solute-solvent energy transfer process, low-frequency modes of proteins seem to be less important.

IX-I-3 Mode Dependence of Vibrational Energy Redistribution in Nickel Tetraphenylporphyrin Probed by Picosecond Time-Resolved Resonance Raman Spectroscopy: Slow IVR to Phenyl Peripherals

MIZUTANI, Yasuhisa; KITAGAWA, Teizo

[*Bull. Chem. Soc. Jpn.* **75**, 965 (2002)]

The formation of the (d , d) excited state of (*meso*-tetraphenylporphyrinato)nickel (II) ([Ni(tpp)]) upon (π , π^*) excitation, and its vibrational energy relaxation were monitored by picosecond time-resolved resonance Raman spectroscopy. Stokes resonance Raman bands due the (d , d) excited state instantaneously appeared upon the photoexcitation into the (π , π^*) excited state. Their intensities decayed with a time constant of about 250 ps, which corresponds to electronic relaxation from the (d , d) excited state to the electronic ground state. This is consistent with the results of ultrafast absorption measurements reported by Eom *et al.* [H. S. Eom, S. C. Jeoung, D. Kim, J. H. Ha and Y. R. Kim, *J. Phys. Chem. A* **101**, 3661 (1997)]. Anti-Stokes ν_4 (macrocycle in-plane mode) intensities of [Ni(tpp)] in the (d , d) excited state appeared promptly and decayed with a time constant of 3.6 ± 0.6 ps. The rise and decay of anti-Stokes intensity are interpreted as vibrational excitation due to the excess energy and intermolecular vibrational energy transfer to the surrounding solvent molecules, respectively. The ϕ_4 mode, which is mainly $\nu(\text{CC})$ of the peripheral phenyl groups, gave no detectable anti-stokes intensity although the mode gave appreciable Stokes intensity. This means that the ϕ_4 mode is left vibrationally less excited than the ν_4 mode in the process of vibrational energy relaxation and that intramolecular vibrational energy redistribution is not completed in a subpicosecond time regime. These results for [Ni(tpp)] demonstrate that the vibrational modes of peripheral groups are vibrationally less excited shortly after the formation of the (d , d) excited state and that energy redistribution in the peripheral groups takes place in picoseconds, such a short time is competitive with vibrational energy transfer to the surrounding solvent molecules.